Characterization of bilayer (FeB/Fe_2B) on AISI H13 work tool steel

Boumaali B.[1], Nait Abdellah Z.[2,1], Keddam M.[1]
[1] Laboratoire de Technologie des Matériaux, USTHB, Algeria
[2] Département de Chimie, Faculté des Sciences, Université Mouloud Mammeri, Algeria
E-mail: mkeddam@usthb.dz

In this work, the borided layers were produced on AISI H13 steel via solid boriding with a powders mixture containing 90 wt.% B_4C and 10 wt.% $NaBF_4$ for treatment times of 2-6 h at 900, 950 and 1000 °C. The microscopic observations revealed a less pronounced toothed interface between the borided layer and the transition zone. The XRD studies indicated the presence of a dual phase boride layer (FeB/Fe_2B) besides the chromium and vanadium borides as precipitates inside it. The boronizing kinetics of AISI H13 steel was investigated by using the classical parabolic growth law. The obtained value of boron activation energy in the entire boride layer ($FeB + Fe_2B$) was found to be 236.34 kJ mol^{-1}. Furthermore, this value of energy has been compared to the literature data. Finally, the nanohardness and reduced modulus of elasticity were measured for FeB, Fe_2B and transition zone.

INTRODUCTION

Boriding is an efficient thermochemical process intended to enhance the surface characteristics of workpieces including the increase in hardness, resistance against wear and corrosion [1]. This thermochemical treatment is achieved between 800 and 1050 °C by varying the exposure time from 0.5 to 10 h. Due to its small atomic radius and high mobility compared to that of iron, the boron element diffuses easily into the steel substrate since its diffusion is a thermally activated process. Thus, the boriding of ferrous materials like steels results in the formation of either a Fe_2B layer or double-layer ($FeB + Fe_2B$). In the case of alloyed steels, the formation of metallic borides is kinetically and thermodynamically possible with the presence of active boron atoms [2-6] at the usual boriding temperatures. The morphology of (boride layer/transition zone) and the proportion of each boride phase depend on various factors such as: the nature of boriding agent, the process temperature, the treatment time and the chemical composition of the material to be thermochemically treated. Among the boriding methods, the pack-boriding process is the preferred one in the industry since it is economical and requires a low investment in equipment [1]. In the industry, the AISI H13 steel finds many applications. For example, it is used to fabricate dies, cutting tools, extrusion tooling and injection molds. It is also characterized by a high hardenability, toughness and good machinability. In order to enhance the tribological performance of AISI H13 steel exposed to extreme wear conditions, the boriding process is needed to get hard boride layers on the surface of this material that meet the wanted requirements in the industry. For this reason, some studies were devoted to the boriding of AISI H13 steels [5, 6, 8-14] under different boriding conditions. For indication, Taktak [5] has pack-boronized the AISI H13 steel in the range of 1073 to 1223 K during 3, 5 and 7 h. The maximum layer thickness of ($FeB + Fe_2B$) was about 45 µm with calculated value of activation energy of 244.37 kJ mol^{-1}. In other paper, Kara et al.[6] have investigated the wear and adhesion behaviour of boride layers on AISI H13 steel at 900 and 950 °C with the exposure times of 2, 4 and 6 h. They have employed the solid boriding with Ekabor 2 as a boriding agent and obtained a layer thickness of ($FeB + Fe_2B$) between 21 ± 3 µm and 85 ± 7 µm. Gunen et al. [8] have analyzed the corrosion resistance of pack-borided AISI H13 steel. They have used a mixture of powders constituting of 95 wt.% B_4C and 5 wt.% $NaBF_4$. Accordingly, the Fe_2B layer was only produced at 800°C while a dual phase boride layer ($FeB+ Fe_2B$) was generated at 900 and 1000 °C. This investigation showed that the corrosion resistance depended on the microstructural nature of the compound layer and its thickness and surface roughness. Karakas et al. [9] have compared the growth kinetics of ($FeB + Fe_2B$) layers formed at the surface of AISI H13 steel by using two boriding agents in the temperature range 800-1000 °C. The first agent was nanosized and had a chemical composition of 90 wt.% amorphous boron and 10 wt.% $NaBF_4$ and the second one was the microsized powders of Ekabor 2. The authors [9] have estimated the values of activation energies in AISI H13 steel in both cases. López-Perrusquia et al. [10] have pack-boronized the AISI H13 steel by the powder method at 1273 K for 8 h using a powders mixture containing B_4C as a boron source and activator KBF_4 where the total boride layer thickness ($FeB + Fe_2B$) reached a value of 139 ± 12 µm. In another work, Campos et al. [11] have used the paste-

boriding process to produce hard boride layers (FeB and Fe_2B) on AISI H13 steel in the temperature of 1173 to 1273 K for exposure times from 2 to 8 h. The boriding agent used was composed of B_4C compound with 76% of boron and cryolite as a main activator. Boonplook et al. [13] have treated the AISI H13 steel by solid boriding using the commercial boriding agent Ekabor I in the range of 1123 to 1173 K during 2,4 and 6 h. In this investigation, the growth kinetics of the dual phase boride layer was analyzed by using an empirical approach. As a result, the activation energy for boron diffusion in AISI H13 steel was estimated as 185.7 kJ mol^{-1} with a maximum layer thickness reaching a value of 66 μm at 1173 K for 6 h.

The aim of the present work was to characterize metallurgically and mechanically the boride layers generated at the surface of AISI H13 steel by employing a powders mixture that guarantee the formation of dual phase boride layer (FeB + Fe_2B) for all boriding conditions. For this reason, the powders mixtures composed of 90 wt.% B_4C and 10 wt.% $NaBF_4$, characterized by high content of high-purity boron carbide were then employed in the present work contrarily to the classical Ekabor powders [1]. Thus, the selected powder mixtures allowed us to give rise to the (FeB/Fe_2B) configuration on AISI H13 steel for the given set of boriding parameters with thicker coatings. The boronizing kinetics of the bilayer (FeB/Fe_2B) produced on AISI H13 steel was investigated. The time dependence of layers's thicknesses was explored in order to deduce the value of boron activation energy in AISI H13 steel when employing the boriding agent with high proportion of boron carbide (90 wt.%). Such a value of energy was contrasted with the literature results. As far as the characterization by nanoindentation of borided AISI H13 steel, up to now there are no studies in the literature about this steel grade. Therefore, the nanomechanical properties of FeB and Fe_2B layers as well as the transient zone were addressed in which the values of nanohardness and reduced modulus of elasticity were determined for FeB, Fe_2B and transition zone by using a peak load of 10 mN.

MATERIAL AND EXPERIMENTAL TECHNIQUES

The AISI H13 steel was employed for pack-boriding experiments. The cut samples with the precision cutting device had a surface area of (35 mm^2) and thickness of 4 mm. Table 1 gives the chemical composition of AISI H13 steel (in weight percent).

Tab. 1. Chemical properties of AA1100

C	Cr	Mo	V	Si	Mn	Fe
0.45	5.25	1.65	1.10	1.0	0.35	balance

Based on the previous studies concerning the boriding of AISI H13 steels [8, 9], a powders mixture of 90 wt% B_4C and 10 wt% $NaBF_4$ having particles' size less than 25 μm was used as the boriding agent. In the previous study by Gunen et. al. [8], the FeB phase was not formed at 800 °C for 2, 4 and 6 h. For this reason, the amount of activator ($NaBF_4$) was increased to 10 wt% in the powders mixture with a boron source of 90 wt.% B_4C in order to ensure the presence of FeB layer at 800 °C whatever the exposure time. Prior to boriding, all the cut samples were grinded with 800-1000-1200 mesh SiC abrasive paper and washed with distilled water, ultrasonically degreased in acetone for 15 minutes and rinsed in alcohol to get a uniform surface. Then the samples were placed in a crucible made of stainless steel with a minimum of 10 mm boron powder on all sides and the top of the crucible was covered 10 mm with 50 wt% Al_2O_3 and 50 wt% Si powders to prevent the oxidation phenomenon at high temperature. Initially, the boriding process was performed at three temperatures 800 °C, 900 °C and 1000 °C for 2, 4 and 6 h [15]. After the completion of the boriding treatment, the borided samples were removed from furnace and cooled to room temperature in air. The same volume crucibles were filled equally in all boriding processes and a fresh boriding powder mixture was used for each boriding process. Since all surfaces are coated in box boriding technique, for metallographic examinations the samples were cut from their middle parts along a surface cross-section with a precision cutting device. Then, the cut surface of the samples was mounted with a hot mounting device to be polished. The mounted surface were ground using 400 to 2000 grit SiC abrasive paper and polished with 1 μm alumina solution to obtain a good mirror finish. After polishing, the samples were etched in a 4 wt.% Nital solution to reveal the microstructure after boriding.

Metallographic studies were carried out on polished and etched cross sections using a Thermo Scientific Apreo S SEM operating at 30 kV, equipped with Thermo TM EBSD (QuasOr) and EDS (UltraDry) detectors (Thermo Fisher Scientific, Waltham, Massachusetts, USA). Since the boride layer is formed as a toothed microstructure, the thickness measurement of boride layer was performed according to method defined by Yu et al. [16], including the boride layer teeth in the calculation. The boride layer thickness was determined by SEM for precise measurement. The presence of phases on the surface of AISI H13 was verified by X-ray diffraction (XRD) analyses utilizing a computer-controlled RIGAKU Smart LabTM (Austin, Texas, USA), for which the operation values were as follows: (Cu-K_α radiation λ = 0.154 nm, 2θ range from 5° to 90°).

Microhardness measurements were performed along the cross-section of the obtained boride layers using a Future-Tech FM-700 hardness tester equipped with a Vickers pyramid indenter with a load of 100 g and a dwell time of 15 s in accordance with the ASTM E384

standard and average of five measurements was taken as the microhardness value of the measured sample.

In addition, the nanoindentation hardness and elastic modulus of obtained boride layers were measured using a Hysitron TI-950 TriboIndenter nanoindenter with a Berkovich tip. The tests were performed in accord with the Oliver-Pharr analysis method using a 3×3 analysis matrix under a peak load of 10 mN [17]. Force-controlled loading was carried out using a trapezoidal function where the load was increased at a constant loading rate in 30 s, held for 10 s and gradually removed in 30 s as stated in the previous studies [18-20]. The measurements were repeated threefold to get an arithmetic mean value. To recall, the nanohardness value (H) of a material is defined as the ratio of maximum load P_{max} to contact area A_c, which is represented by:

$$H = \frac{P_{\max}}{A_C} \tag{1}$$

The contact depth h_c is calculated using Equation (2):

$$h_C = h_{\max} - \varepsilon \frac{P_{\max}}{S} \tag{2}$$

where h_{max} is the maximum depth and S is relative to the slope of the unloading curve ($S = dP/dh$). Since a Berkovich probe was used in this study, the value of ε was taken as 0.753. The reduced or effective elastic modulus E_r is calculated from Equation (3):

$$\frac{1}{E_r} = \frac{1-\upsilon_S^2}{E_S} + \frac{1-\upsilon_i^2}{E_i} \tag{3}$$

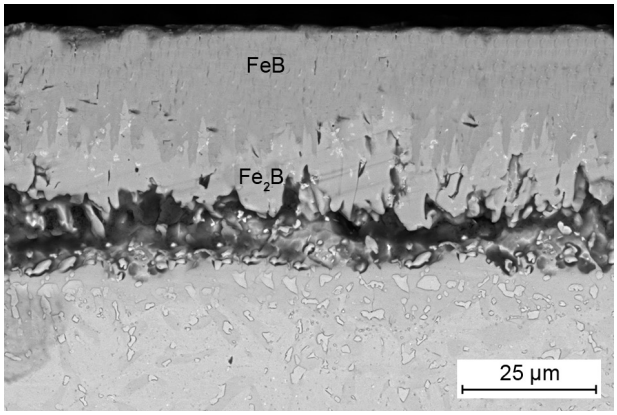
where E_s and υ_s are Young's modulus and Poisson's ratio, respectively. In Equation (3), the subscript s represents the sample and i refers to the Berkovich indenter. In a conventional nanoindentation measurement, the reduced elastic modulus is determined from the slope of the discharge curve at maximum load, using Equation (4):

$$E_r = \frac{\sqrt{\pi}\, S}{2\sqrt{A_C}} \tag{4}$$

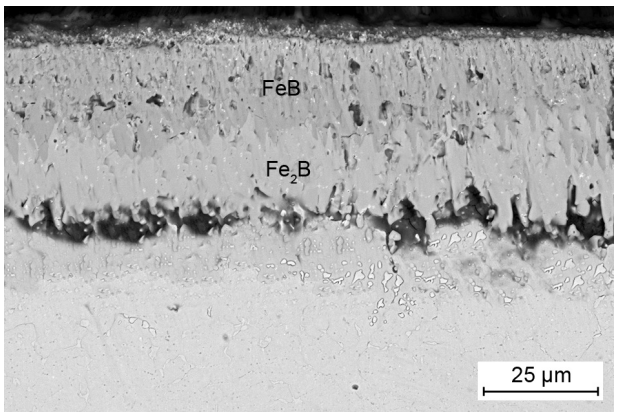
EXPERIMENTAL RESULTS AND DISCUSSIONS:

SEM observations of boride layers

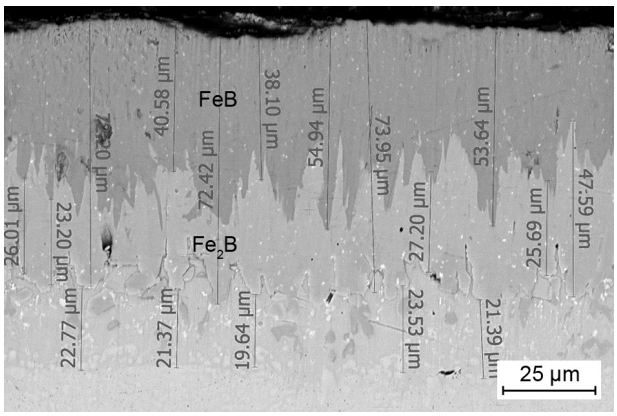
Figure 1 shows the SEM micrographs of the cross-sectional views of boride layers produced on the surfaces of AISI H13 steels for different boriding parameters. The boride layers looks dense, continuous and compact for all boriding conditions with the interfaces having a less toothed shape due to the presence of alloying elements such as Cr, V and Mo in the AISI H13 steel. It is recognized that the alloying elements have a strong impact on the development of flat interfaces as seen in some borided alloyed steels [21-24]. In fact, the presence of high ratio of alloying elements diminished the active flux of boron atoms and had a strong tendency to flatten the interfaces between the boride layers and the transition zone. This latter zone which is visible in (Figs. 1a,b) contains insoluble elements being pushed away from the diffusion front. The thickness of boride layer reached a value of 38 ± 3.5 µm at 900 °C for 4 h and a value of 130 ± 8.2 µm at 1000 °C during 6 h.



a) 900 °C for 4 h

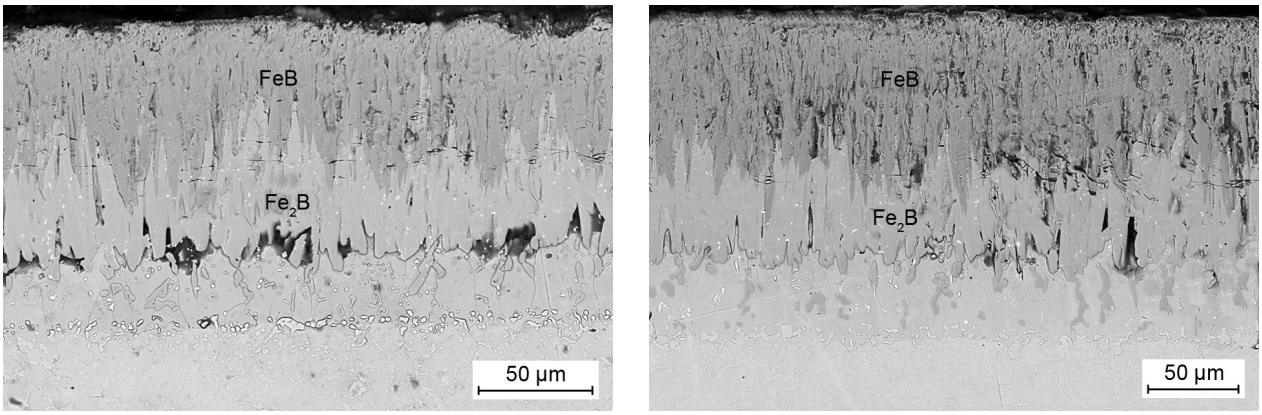


b) 950 °C for 2 h



c) 1000 °C for 2 h

Fig. 1. SEM micrographs of the cross sections of boronized AISI H13 steel according to different boriding conditions: a) 900 °C for 4 h, b) 950 °C for 2 h, c) 1000 °C for 2 h *(Continue on next page)*



d) 1000 °C for 4 h e) 1000 °C for 6 h

Fig. 1. SEM micrographs of the cross sections of boronized AISI H13 steel according to different boriding conditions: d) 1000 °C for 4 h, e) 1000 °C for 6 h

XRD analysis

Figure 2 displays the XRD patterns obtained on the surfaces of pack-boronized AISI H13 steel at 1000 °C for increasing exposure times (2, 4 and 6 h). The XRD analyzes showed the presence of dual phase boride layer composed of two types of iron borides (FeB and Fe_2B) besides two types of metallic borides (VB and Cr_6B_5) because of chemical affinity of alloying elements to boron element. The presence of other types of metallic borides on treated AISI H13 steels [5,25] are related to different boriding conditions in terms of nature of process, the nature of boriding agent and also the boriding temperature and the treatment time. For instance, Kara et al. [6] have identified on the surface of AISI H13 steel boronized at 900 and 950 °C for 4, the presence of CrB phase using Ekabor 2 powder as boronizing agent. The same metallic boride (CrB) was also detected by XRD analysis by Taktak [5, 25] when boriding the AISI H13 steel by salt-bath method at 1173 K for 5 h.

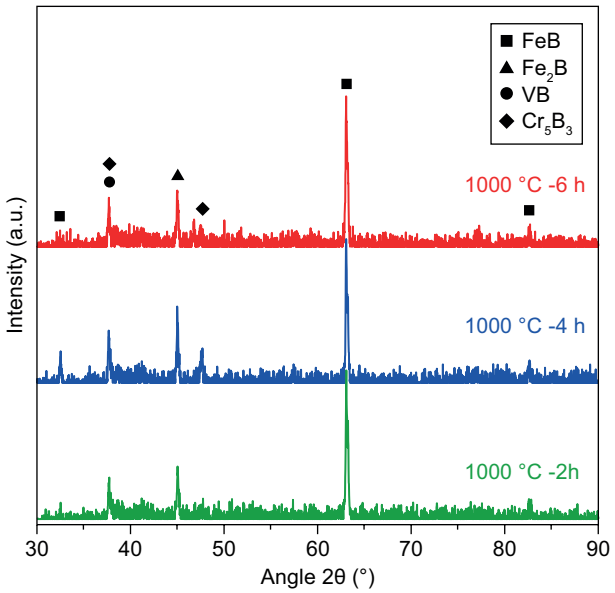


Fig. 2. XRD patterns recorded at the surfaces of borided AISI H 13 steel

Nanoindentation results

Figure 3 provides the nanoindentation curves for two borided samples at 1000 °C for 4 and 6 h, respectively. Three indents in each region (FeB, Fe_2B and transition zone) were done on the cross-sections of the treated samples to determine the values of reduced Young modulus and the corresponding values of nanohardness. Figure 4 shows the images of indentation marks left on the surfaces of FeB and Fe_2B zones along the cross-section of boronized AISI H13 steel at 1000 °C for 6 h. The data from Figure 3 were used to get the numerical values of reduced modulus of elasticity and nanohardness which are gathered in Table 2.

It is seen that the nanohardness values are depending on both the treatment time and the nature of phases at 1000 °C. The nanohardness of FeB is slightly higher than that of Fe_2B because of strong bonds between boron and iron atoms within the FeB crystalline structure. The transition zone possesses a lower value of nanohardness in comparison to the FeB and Fe_2B layers. It should be mentioned that the values of nanohardness are affected by the occurrence of residual stresses generated in the borided AISI D2 steel after cooling [26]. The values of reduced modulus of elasticity ranged from 150.39 to 160.15 GPa for FeB, between 148.02 and 151.76 GPa for Fe_2B and 106.23 GPa for the transient zone. The values of nanohardness are determined as 19.24-21.27 GPa for FeB, 14.8-18.31 GPa for Fe_2B and 5.9 GPa for the transient zone.

Concerning other findings about the nanomechanical properties of borided steels, Culha et al.[27] have determined the elastic modulus values (in the range of

Tab. 2. Values of nanohardness and reduced modulus of elasticity measured in the three regions (FeB layer, Fe2B layer and transition zone) for two borided samples at 1000 °C for 4 and 6 h

Measurements	**FeB layer**	**Fe_2B layer**	**Transition zone**
Average nanohardness (GPa) For the 4 h borided sample	21.27	14.8	5.90
Reduced modulus of elasticity (GPa) For the 4 h borided sample	160.15	151.76	106.24
Average nanohardness (GPa) For the 6 h borided sample	19.24	18.31	5.90
Reduced modulus of elasticity (GPa) For the 6 h borided sample	150.39	148.02	106.24

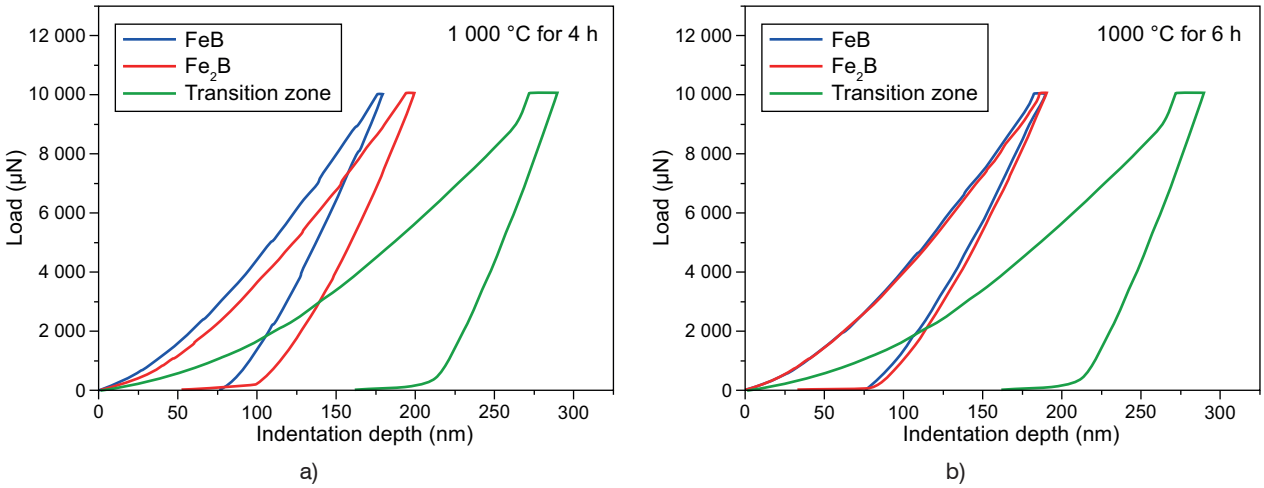
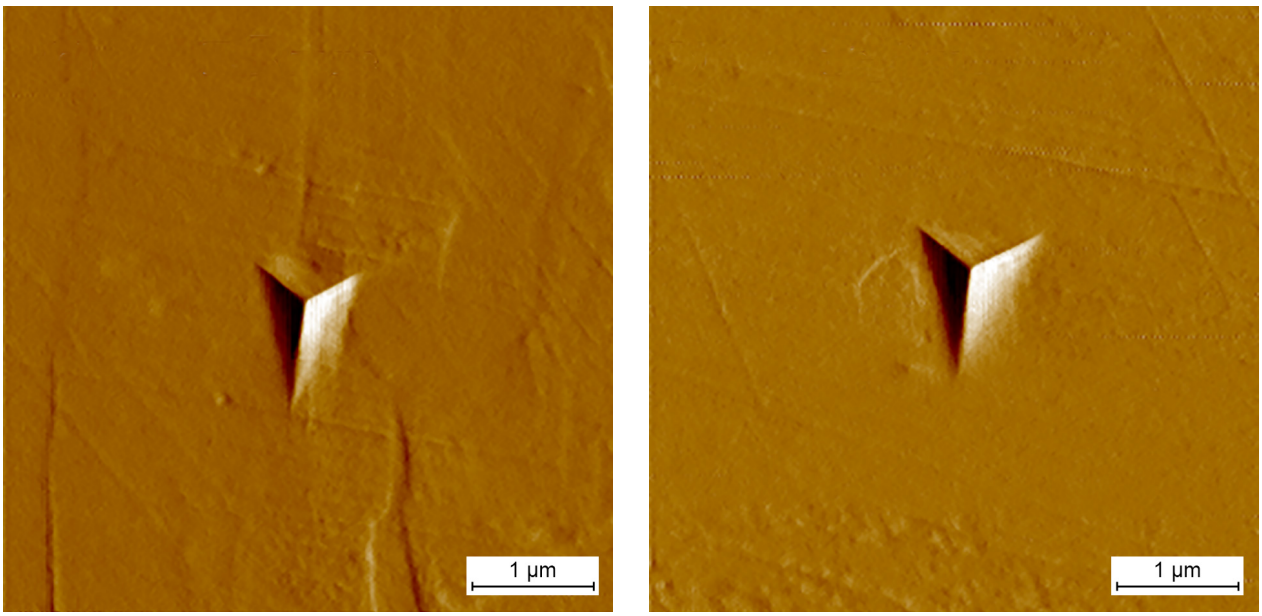


Fig. 3. Curves of nanoindentation tests for the boronized AISI H13 steels at 1000 °C for two exposure times: a) 4 h, b) 6 h



a) FeB zone b) Fe_2B zone

Fig. 4. Images of indentation marks left on the indented surfaces of the cross-sections of borided AISI H13 steel at 1000°C for 6 h in two different locations: a) FeB zone; (b Fe_2B zone

125-397 GPa) for the FeB layer by using the nanoindentation tests on AISI 1020 and AISI 1040 steels and by varying the peak load between 80 and 640 mN. In that experimental work, the measured elastic modulus exhibited a strong peak load dependency.

In other study, Rodríguez-Castro et al. [28] have also estimated the nanomechanical properties by using Berkovich nanoindentation tests (under two loads 500 and 1000 mN) in the Fe_2B layer and the diffusion zone for AISI 1045 steels borided at 1223 K for 1 and 3 h with and without post-heat treatment. The nanohardness values of Fe_2B layer were in the range of 18.3 to 18.7 GPa whilst the elastic modulus values were found between 285 and 300 GPa. For the diffusion zone, the corresponding values were in the range of 4.4-9.6 GPa for the nanohardness values and 235-255 GPa for the elastic module values. In addition, it was reported that the post heat treatment after boriding of AISI 1045 steels had a positive impact on nanomechanical properties by lowering the hardness gradient between the Fe_2B layer and the substrate. Kulka et al. [29] have gas borided the Armco iron substrate at 920 °C for 3 h and performed the nanoindentation tests with Berkovich indenter with a maximum load of 50 mN. For the FeB region, the measured elastic modulus was 308.86 GPa with a nanohardness of 20.95 GPa. The Fe_2B region had an elastic modulus value of 252.96 GPa with a nanohardness of 17.42 GPa. These results in terms of elastic modulus contrasted with the present experimental measurements performed in this study with a maximum load of 10 mN obtaining the values of reduced elastic modulus in the range 150.39-160.15 GPa for FeB, and in the range 148.02-151.76 GPa for Fe_2B and 106.23 GPa for the transition zone. It can be concluded that the measured values of elastic modulus and nanohardness depended on the peak load used and on the post-treatments applied to borided steels. However, the obtained values of nanohardness in the present work are consistent with the literature data [26, 27-29].

Microhardness measurements

Table 3 gives the microhardness values determined along the cross-sections of boronized layers. The microhardness values for FeB layer are in the range of 2000-2700 $HV_{0.1}$ while those of Fe_2B are between 1850 and 2600 $HV_{0.1}$ depending on the boriding parameters. Particularly, at 1000 °C for 4 and 6 h, the microhardness values of FeB are 2600 and 2700 $HV_{0.1}$ (i.e. 26 and 27 GPa), respectively. These values are slightly higher compared to the nanohardness results displayed in Table 2.

The same situation was observed for the values of nano and microhardness obtained at 1000 °C for 4 and 6 h. This slight difference between nano and microhardness values can be attributed to the use of projected contact area at peak load and the extent of plastic zone under the indenter during the measurements from the nanoindentation curves. It is noticed that the microhardness values are decreased with the diffusion depth and attained a value ranged from 460 to 600 $HV_{0.1}$ for the matrix. These findings are in line with the results reported on borided AISI H13 steels by Kara et al. [6]. Furthermore, the microhardness values measured in the diffusion zone are between 820 and 580 $HV_{0.1}$.

Kinetic study

The growth kinetics of entire boride layer on AISI H13 steel has been investigated by plotting its thickness versus the square root of treatment time for increasing temperatures according to Equation (5) [30-33].

$$u = k\sqrt{t} = \sqrt{Dt} \tag{5}$$

The term u is the entire boride layer thickness and D the diffusion coefficient of boron and t the treatment time. The boronizing kinetics is governed by the diffusion of boron atoms into the substrate to produce hard boride layer at the material surface. In Table 4 are listed the experimental layers' thicknesses of (FeB + Fe_2B) depending on the boriding parameters (the boriding temperature and the treatment time).

Tab. 3. Values of microhardness along the cross-sections of boronized layers on AISI H13 steel

Boriding conditions	FeB layer	Fe_2B layer	Diffusion zone	Matrix near diffusion zone	Matrix
900 °C, 2 h	2000	2000	580	480	460
900 °C, 4 h	2400	1850	500	460	460
900 °C, 6 h	2450	1900	530	460	460
950 °C, 2 h	2200	2000	750	470	470
950 °C, 4 h	2050	1850	820	530	550
950 °C, 6 h	2500	2500	600	530	550
1000 °C, 2 h	2500	2500	650	600	600
1000 °C, 4 h	2600	2600	750	540	540
1000 °C, 6 h	2700	2400	730	560	560

Tab. 4. Experimental values of entire boride layer thickness for all boriding conditions

Boriding conditions	Experimental entire boride layer thickness (µm)
900°C, 2 h	25 ± 3.1
900°C, 4 h	38 ± 3.5
900°C, 6 h	55 ± 4.6
950°C, 2 h	46 ± 4.8
950°C, 4 h	60 ± 5.7
950°C, 6 h	75 ± 6.1
1000°C, 2 h	70 ± 5.3
1000°C, 4 h	110 ± 7.5
1000°C, 6 h	130 ± 8.2

By plotting the entire boride layer thickness as a function of square root of time, it is possible to deduce the values of parabolic growth constants at 900, 950 and 1000 °C given in Table 5.

Tab. 5. Experimental parabolic growth constants in the temperature range 900-1000 °C

Temperature (°C)	Experimental parabolic growth constant k (µm $s^{-0.5}$)
900	0.3437
950	0.5121
1000	0.8853

Figure 5 describes the temperature dependence of boron diffusion coefficient through the entire boride layer. Each value of boron diffusion coefficient is the square of the corresponding parabolic growth constant according to Equation (5). The slope of the obtained straight line corresponds to the value of boron activation energy (= 235.76 kJ mol^{-1}) for AISI H13 steel.

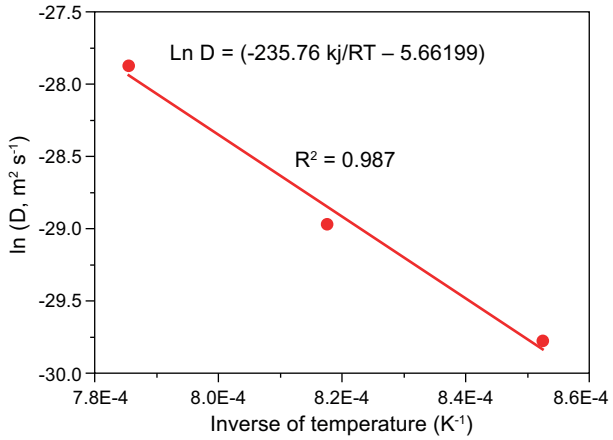


Fig. 5. Arrhenius relationship relating the boron diffusion coefficient in the dual phase boride layer to the boriding temperature

Figure 6 compares the simulated values of entire boride layer with the predicted values by Equation (5). It is noticed that the predicted values of layers' thicknesses are in line with the experimental data. Equation (5) can be utilized as a simple tool to select the optimum value of entire boride layer thickness for potential industrial applications.

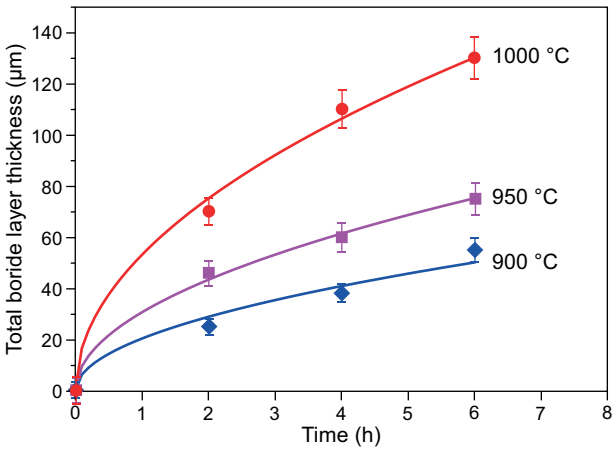


Fig. 6. Evolution of boride layer thickness as a function of treatment time. Continuous lines represent the simulated results and the symbols are the obtained experimental data

Table 6 gives a comparison between the value of activation energy estimated in this work and the values taken from the literature [9,11,13,34, 35] for boronized AISI H13 steels. It is noticed that the reported values of activation energies were very comparable for the paste and powder methods.In this respect, Karakas et al. [9] have pack-boronized the AISI H13 steel between 1073 and 1273 K during 2, 4 and 6 h by using two different boriding agents (commercial Ekabor 2 and nano-sized boron (NB)). The entire boride layer reached a thickness of 103.8 µm for nano-sized boron and 96.5 µm for Ekabor 2. it is concluded that the growth kinetics of boride layers was increased when employing nano-sized boron due to the increase in the surface energy of nano-powders used, resulting into a thermal activation of boron diffusion. Consequently, the calculated activation energy (= 227.5 kJ mol^{-1}) for the process is lower in comparison with the the value obtained (= 284.2 kJ mol^{-1}) when using the Ekabor 2 as boronizing agent. Campos-Silva et al. [11] have proposed a mathematical model based on the modified form of mass balance eqautions at the two growing interfaces (FeB/Fe_2B) and (Fe_2B/substrate) in order to assess the boron diffusion coefficients in FeB and Fe_2B. The calculated values of boron activation energies are resepctively 219.2 and 189.6 kJ mol^{-1} for FeB and Fe_2B due to the efect of alloying elements mainly chromium and vanadium in the AISI H13 steel. In other investigation, Taktak [5] have borided the AISI H13 steel in slurry salt bath containing borax, boric acid, and ferrosilicon in the range of 800 to 950 °C during

Tab. 6. Comparsion of the calculated activation energy with the values reported in the literature for borided AISI H13 steels

Steel	Boriding method	Temperature range (°C)	Activation eenrgy (kJ mol^{-1})	References
AISI H13	Powder	800-1000	227.5 ($FeB+Fe_2B$) with Nanoboron (NB) 284.2 ($FeB+Fe_2B$) with Ekabor II	[9]
AISI H13	Paste	900-1000	219.2 (FeB), 189.6 (Fe_2B)	[11]
AISI H13	Powder	850-950	185.7 ($FeB+Fe_2B$)	[13]
AISI H13	Powder	800-1000	186.2 ($FeB+Fe_2B$)	[34]
AISI H13	Powder	850-1000	233 (Fe_2B)	[35]
AISI H13	Powder	900-1000°C	235.76 ($FeB+Fe_2B$)	Present work

treatment times of 3, 5, and 7 h. They have obtained a dual phase boride layer with a thickness ranging from 8 to 58 μm with the estimated parabolic growth constant of 0.365 μm $s^{-0.5}$ at 950 °C. By comparison of this value with that of obtained in our experiments, it can be concluded that the boriding kinetics of AISI H13 steel is directly influenced by the choice of boriding method.

CONCLUSIONS

In this study, the AISI H13 steel has been successfully boronized in the range of 800 to 1000 °C for treatment times of 2-6 h. The SEM examinations showed the occurrence of two types of layers (the outer one: FeB and the inner one: Fe_2B) with a visible transient zone. The thickness of dual phase boride layer ranged between 25 ± 3.1 and 130 ± 8.2 μm with a less toothed morphology. Furthermore, the XRD analyses confirmed the presence of iron borides (FeB and Fe_2B) and metallic borides of type Cr_5B_3 and VB as precipitates due to the chemical affinity of boron to the transition metals Cr and V. The measured values of microhardness ranged from 2000 to 2700 $HV_{0.1}$ for the FeB layer, between 1850 and 2600 $HV_{0.1}$ for the Fe_2B layer, from 820 to 580 $HV_{0.1}$ for the diffusion zone and in the range of 460-600 $HV_{0.1}$ for the matrix. The values of modulus of elasticity and nanohardness were measured in three regions (FeB, Fe_2B and transition zone) for two borided samples at 1000 °C for 4 and 6 h. As a result, the values of reduced modulus of elasticity ranged from 150.39 to 160.15 GPa for FeB, between 148.02 and 151.76 GPa for Fe_2B and 106.23 GPa for the transition zone. The determined values of nanohardness were 19.24-21.27 GPa for FeB, 14.8-18.31 GPa for Fe_2B and 5.9 GPa for the transition zone. The boronizing kinetics of AISI H13 steel is ruled by the parabolic growth law with a value of activation energy for boron diffusion equal to 235.76 kJ mol^{-1}. This value of activation energy can be explained by the effect of alloying elements in AISI H13 steel on the diffusion rate of boron atoms resulting from a source with high proportion of B_4C compound. In addition, the obtained value of boron activation energy in AISI H13 steel was consistent with the results derived from the literature [9, 11, 13, 34, 35].

REFERENCES

1. Kulka M. *Trends in thermochemical techniques of boriding*, in: Current Trends in Boriding, Engineering Materials. Springer: Cham, Switzerland, **2019**.
2. Sen U., Sen S., The fracture toughness of borides formed on boronized cold work tool steels, *Materials Characterization* **2003**, 50, 261-267.
3. Dokumaci E., Özkan I., Önay B., Effect of boronizing on the cyclic oxidation of stainless steel, *Surface and Coatings Technology* **2013**, 232, 22-25.
4. Keddam M., Chegroune R., Kulka M., Makuch N., Panfil D., Siwak P., Taktak S., Characterization, tribological and mechanical properties of plasma paste borided AISI 316 steel, *Transactions of the Indian Institute of Metals* **2018**, 71, 79-90.
5. Taktak S., Some mechanical properties of borided AISI H13 and 304 steels, *Materials and Design* **2007**, 28, 1836–1843.
6. Kara R., Çolak F., Kayali Y., Investigation of Wear and Adhesion Behaviors of Borided Steels, *Transactions of the Indian Institute of Metals*, **2015**, 69, 1169–1177.
7. Hudáková M., Jurči P., Microstructure and Microhardness of Powder Boronized Vanadis 6 Steel. *Defect and Diffusion Forum* **2019**, 395, 73–84.
8. Günen A., Karahan I.H., Karakaş M.S., Kurt B., Kanca Y., Çay V.V., Yıldız M., Properties and Corrosion Resistance of AISI H13 Hot-Work Tool Steel with Borided B_4C Powders, *Metals and Materials International* **2020**,26, 1329–1340
9. Karakaş M.S., Günen A., Kanca E., Yilmaz E., Boride layer growth kinetics of AISI H13 steel borided with nano-sized powders. Archives of Metallurgy and Materials, *Archives of Metallurgy and Materials* **2018**, 63, 159-165.
10. López-Perrusquia N., Campos-Silva I., Martínez-Trinidad J., Avilés A., Alvárez-Castañeda E., Juárez-Torres S., Evaluation of Brittle Layers Obtained by Boriding on AISI H13 Steels, *Advanced Materials Research* **2009**, 65, 47–52.
11. Campos-Silva I., Ortíz-Domínguez M., López-Perrusquia N., Escobar Galindo R., Gómez-Vargas O.A., Hernández-Sánchez E., Determination of Boron Diffusion Coefficients in Borided Tool Steels. *Defect and Diffusion Forum* **2009**, 283-286, 681–686.
12. Vega-Morón R.C., Rodríguez-Castro G.A., Jiménez-Tinoco L.F., Meneses-Amador A., Méndez-Méndez J.V., Escobar-Hernández J., Reséndiz-Calderón C.D., Nava-Sánchez J.L., Multipass Scratch Behavior of Borided and Nitrided H13 Steel, *Journal of Materials Engineering and Performance* **2018**, 27, 3886–3899.

13. Boonplook Y., Juijerm P., Prediction of Boride Thickness on Tool Steels AISI D2 and AISI H13 Using Boriding Kinetics, *Advanced Materials Research* **2014**, 931-932, 296–300.
14. López-Perrusquia N., Doñu-Ruíz M.A., Vasquez F., Trujillo-Alfaro O., Vargas-Oliva Y.E., Study of Adhesion in Steels Surface Hardened, *Advanced Materials Research* **2012**, 535-537, 513–516.
15. Nait Abdellah Z., Boumaali B., Keddam M., Experimental evaluation and modelling the boronizing kinetics of AISI H13 hot work tool steel, *Materials Testing* **2021** (in press).
16. Yu L.G., Khor K.A., Sundararajan G., Boriding of mild steel using the spark plasma sintering (SPS) technique, *Surface and Coatings Technology*, **2002**, 157, 226-230.
17. Oliver W.C., Pharr G.M., An improved technique for determining hardness and elastic modulus using load and displacement sensing indentation experiments, *Journal of Materials Research*, **1992,** 7, 1564–1583.
18. Oliver W.C., Measurement of hardness and elastic modulus by instrumented indentation: Advances in understanding and refinements to methodology, *Journal of Materials Research* **2004**, 19, 3-20.
19. Günen A., Kalkandelen M., Gök M.S., Kanca E., Kurt B., Karakaş M.S., Karahan I.H., Çetin M., Characteristics and high temperature wear behavior of chrome vanadium carbide composite coatings produced by thermo-reactive diffusion, *Surface and Coatings Technology* **2020**, 420, 126402.
20. Demir, M., Kanca E., Karahan I.H., Characterization of electrodeposited Ni–Cr/hBN composite coatings, *Journal of Alloys and Compounds* **2020**, 844, 155511.
21. Lakhtin Y.M., Pchelkina M.A., Boronizing of high-alloy steels, *Met Sci Heat Treat*, **1961**, 3, 111-114.
22. Campos-Silva I., Ortiz-Domínguez M., Tapia-Quintero C., Rodríguez-Castro G., Jiménez-Reyes M.Y., Chávez-Gutiérrez E., Kinetics and Boron Diffusion in the FeB/Fe_2B Layers Formed at the Surface of Borided High-Alloy Steel, *J of Mater Eng and Perform* **2012,** 21, 1714–1723.
23. Ayvaz S.I., Aydin I., Effect of the Microwave Heating on Diffusion Kinetics and Mechanical Properties of Borides in AISI 316L, *Trans Indian Inst Met* **2020,** 73, 2635–2644.
24. Mejía-Caballero I., Escobar-Martínez C., Palomar-Pardavé M., Le Manh L., Romero-Romo M., Rodríguez-Clemente E., Lartundo-Rojas L., Campos-Silva I., On the Corrosion Mechanism of Borided X12CrNiMoV12-3 Steel Immersed in a Neutral Aqueous Solution Containing Chloride and Sulfate Ions, *Metallurgical and Materials Transactions A*. **2020**, 51, 4868–4879.
25. Taktak S., A study on the diffusion kinetics of borides on boronized Cr-based steels, *Journal of Materials Science* **2006**, 41, 7590–7596.
26. Rodríguez-Castro G., Campos-Silva I., Chávez-Gutiérrez E., Martínez-Trinidad J., Hernández-Sánchez E., Torres-Hernández A., Mechanical properties of FeB and Fe_2B layers estimated by Berkovich nanoindentation on tool borided steel, *Surface and Coatings Technology* **2013**, 215, 291–299.
27. Culha O., Toparli M., Sahin S., Aksoy T., Characterization and determination of Fe_xB layers' mechanical properties, *J. Mater. Process. Technol.* **2015**, 206, 231-240.
28. Rodríguez-Castro G., Campos-Silva I., Martínez-Trinidad M., Figueroa-López. U., Rodríguez-Pulido A., Hernández-Sánchez E., Hernández-Sánchez J., Mechanical behaviour of AISI 1045 steels subjected to powder-pack boriding , *Kovove Mater* **2012**, 50, 357-364.
29. Kulka M., Makuch, N., Piasecki, A., Nanomechanical characterization and fracture toughness of FeB and Fe_2B iron borides produced by gas boriding of Armco iron, *Surface and Coatings Technology* **2017**, 325, 515-532.
30. Bouarour B., Keddam M., Allaoui O., Azouani O., Boriding kinetics of C35 steel: estimation of boron activation energy and the mass gain, *Metallurgical Research and Technology* **2014**, 111, 67-73.
31. Sen S., Sen U., Bindal C., The Growth Kinetics of Borides Formed on Boronized AISI 4140 Steel, *Vacuum* **2005**, 77, 195–202.
32. Azouani O., Keddam M., Allaoui O., Sehisseh A., Kinetics of formation of boride layers on EN-GJL-250 gray cast iron, *Materials Performance and Characterization* **2017**, 6, 510-522.
33. Azouani O., Keddam M., Allaoui O., Sehisseh A., Kinetic Analysis of pack-borided gray cast iron*, Materials Performance and Characterization* **2021**, 10, 226-236.
34. Genel K., Boriding kinetics of H13 steel, *Vacuum* **2006**, 80, 451–457.
35. Keddam M., Ortiz-Dominguez M., Elias-Espinosa M., Damian-Mejia O., Arenas-Flores A., Gomez-Vargas O.A., Abreu-Quijano M., Aldana-Gonzalez J.I, Zuno-Silva J, Growth Kinetics of the Fe_2B Coating on AISI H13 Steel, *Trans. Indian Inst. Met*. **2015**, 68, 433-442.